

**Tuning functional substituent group and guest of
metal–organic frameworks in hybrid membranes for
improved interface compatibility and proton conduction**

Xi-Yan Dong,^{a,b} Jing-Juan Li,^b Zhen Han,^b Pei-Gao Duan,^a Lin-Ke Li^{*,b} and Shuang-Quan Zang^{*,b}

^aCollege of Chemistry and Chemical Engineering, Henan Polytechnic University, Jiaozuo 454000, China.

^bCollege of Chemistry and Molecular Engineering, Zhengzhou University, Science Road No. 100, Zhengzhou 450001, China.

*To whom correspondence should be addressed. E-mail: zangsqzg@zzu.edu.cn;

To test the stability of MIL-101 to acid used in our experiment, we sufficiently washed acid@MIL101 (H_2SO_4 and HNO_3) using water for acid elimination. For the restored MIL-101 from acid-loaded samples, the PXRD patterns are well consistent with those of the pristine MIL-101, even if we used concentrated HNO_3 (Figs. 1–4)

To address the issue about the stability of MIL-101 in the composite, we nitrated some hybrid membranes that were prepared one year before using concentrated HNO_3 at 60°C . The recollected precipitation was centrifuged and washed by water, the obtained powder samples was the recovered-MIL-101 from hybrid membrane (containing some fragments of CS membrane), which was then characterized by PXRD measurement (Fig. S2). The results demonstrate the recovered-MIL-101 from hybrid membrane retain the same structure with pristine MIL-101, and it could not be destroyed by acid in our experiments.

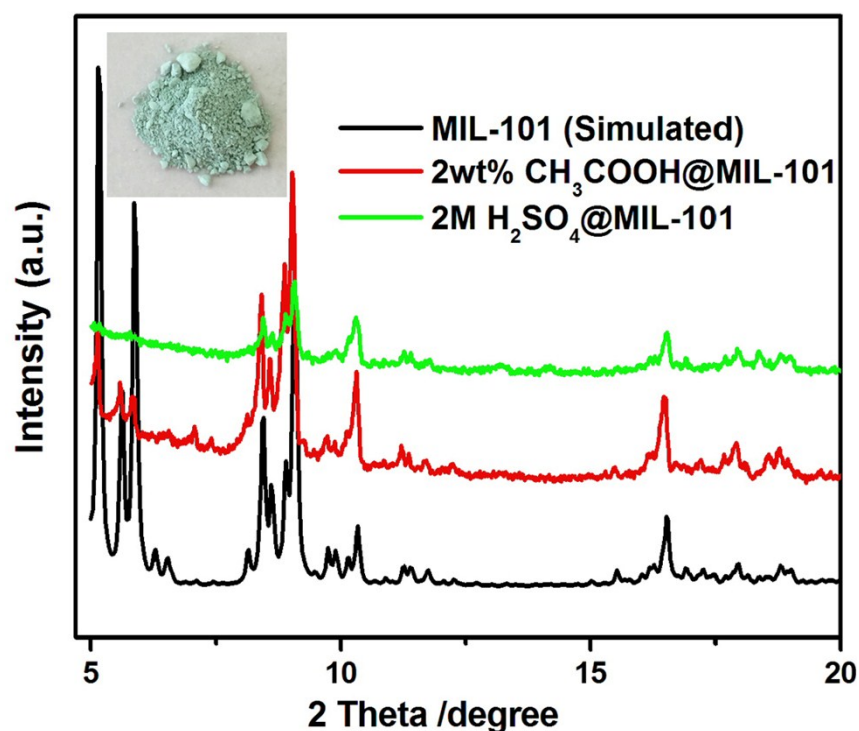


Fig. S1 Comparison of PXRD patterns of acid-treated MIL-101 with that of the simulated MIL-101.

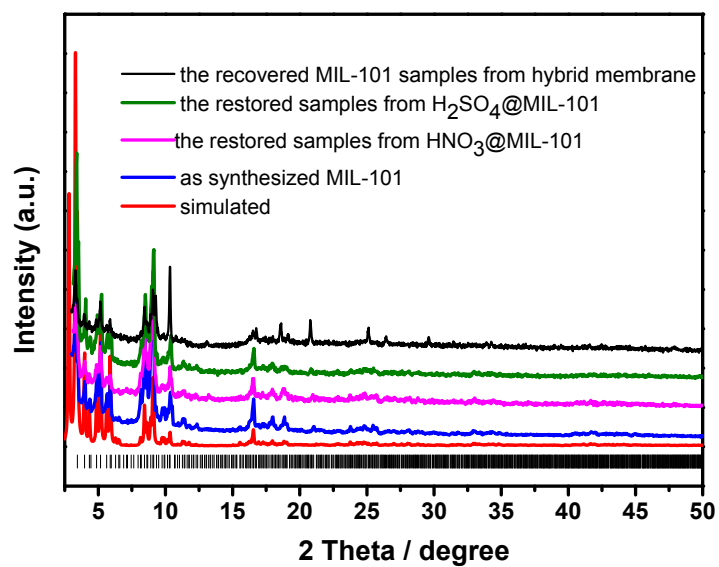


Fig. S2 PXRD patterns of as synthesized crystals, the restored MIL-101 from HNO₃@MIL101 samples, the restored MIL-101 from H₂SO₄@MIL101 samples and the recovered-MIL-101 samples from hybrid membrane.

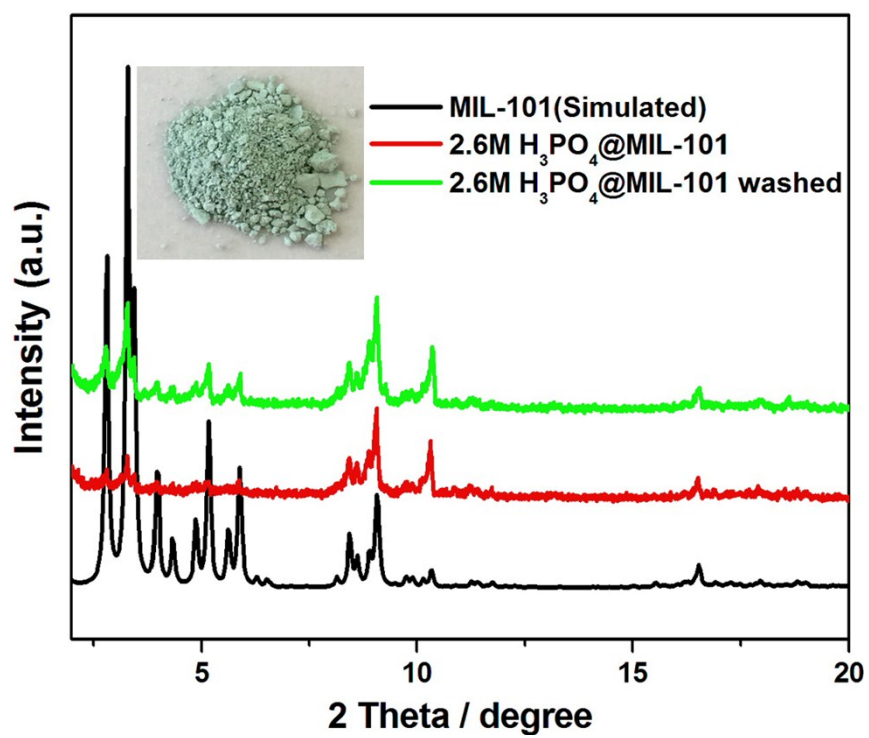


Fig. S3 Comparison of PXR D patterns of experimental H₃PO₄@MIL-101 with that of the simulated MIL-101.

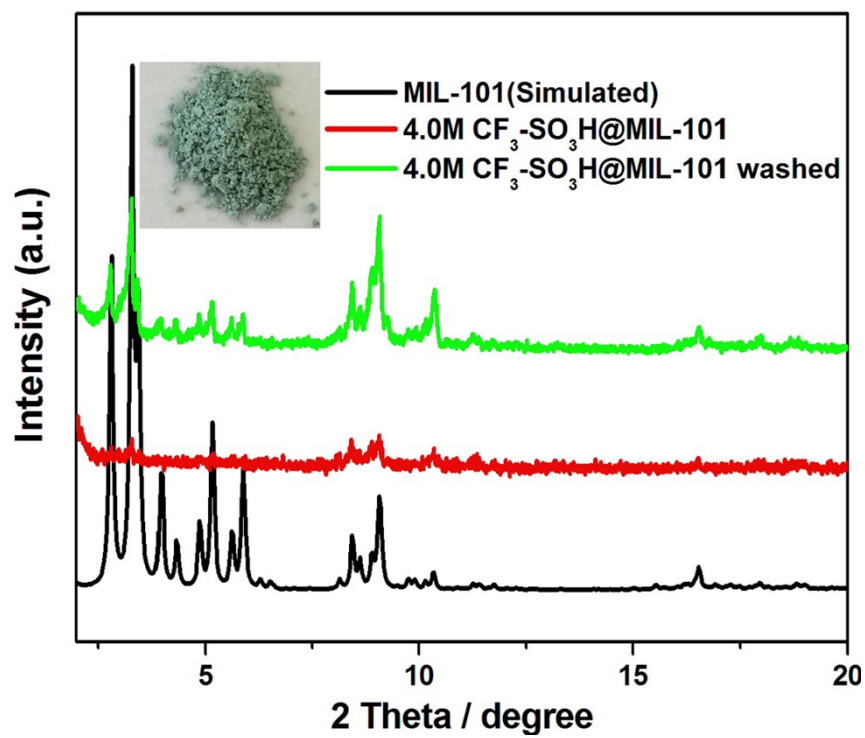


Fig. S4 Comparison of PXR D patterns of experimental CF₃SO₃H@MIL-101 with that of the simulated MIL-101.

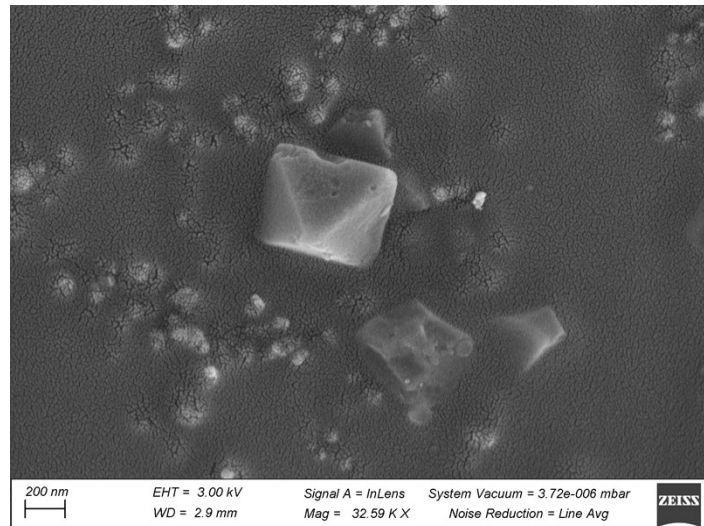
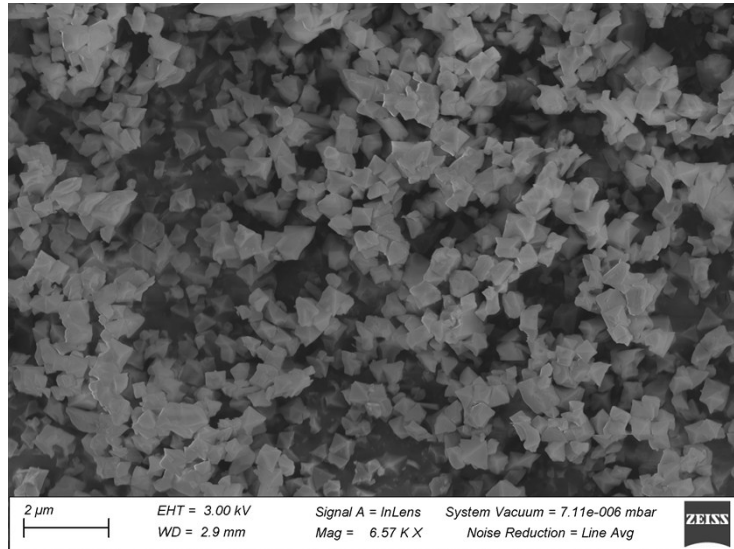


Fig. S5 SEM images of the restored MIL-101 from acid-loaded samples by complete water washing. In contrast to Fig 2, the acid treatment did not obviously damage their original morphology.

To further confirm its structural stability, we performed nitrogen sorption measurements at 77 K (Fig S6, see below), which gave the overlapping adsorption isotherm for the pristine MIL-101 and the restored MIL-101 from acid-loaded samples, suggesting that its host framework and pore structure retained and were not affected by acid treatment.

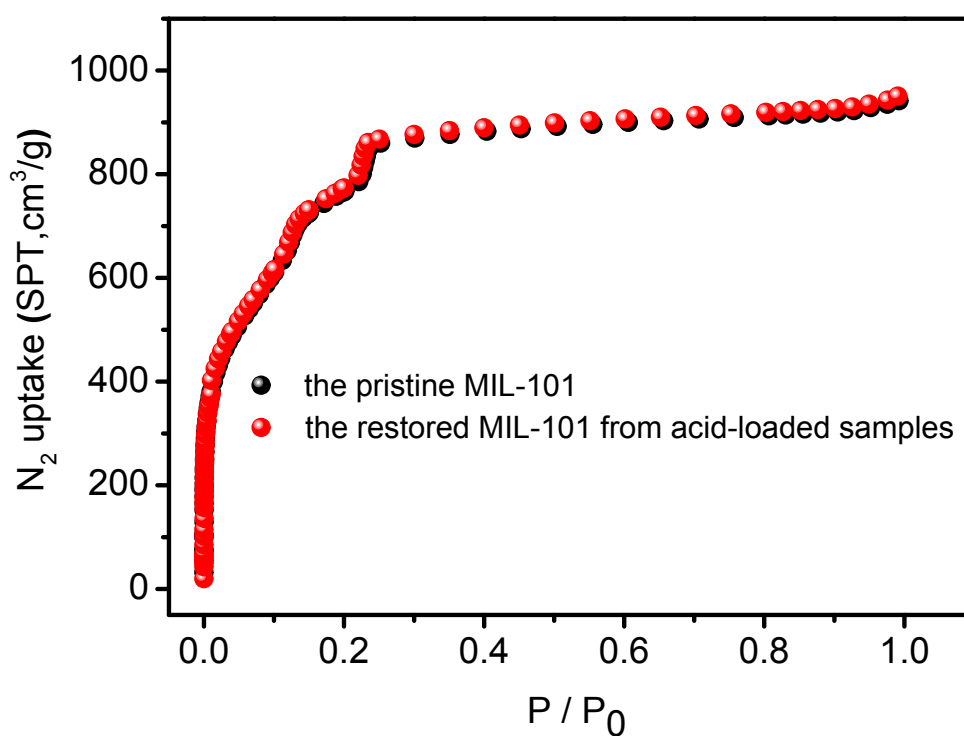


Fig. S6. N₂ sorption isotherm for pristine MIL-101 and the restored MIL-101 from acid-loaded samples at 77 K.

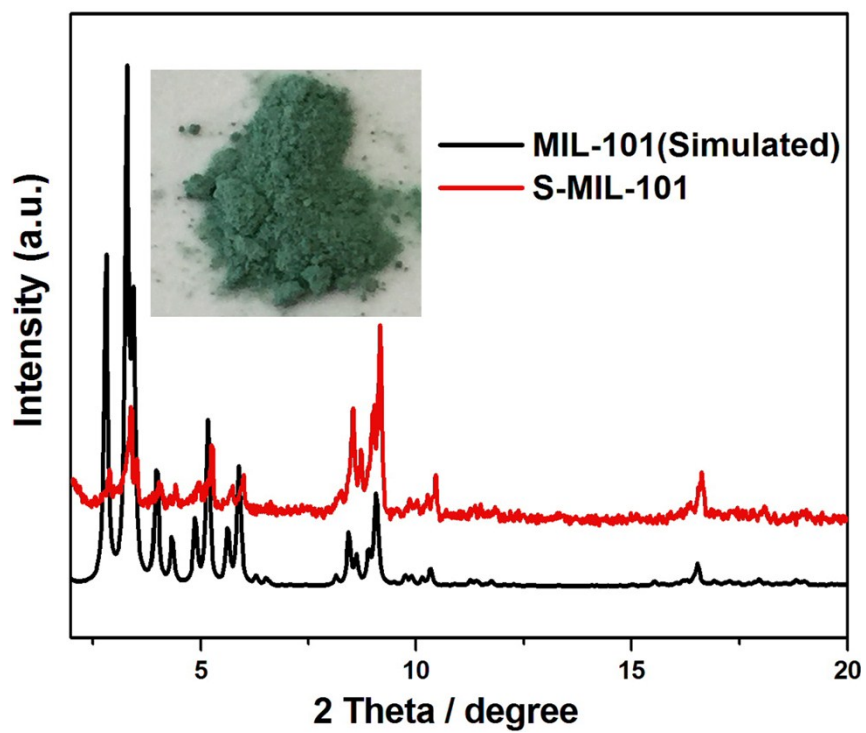


Fig. S7 Comparison of PXRd patterns of experimental S-MIL-101 with that of the simulated MIL-101.

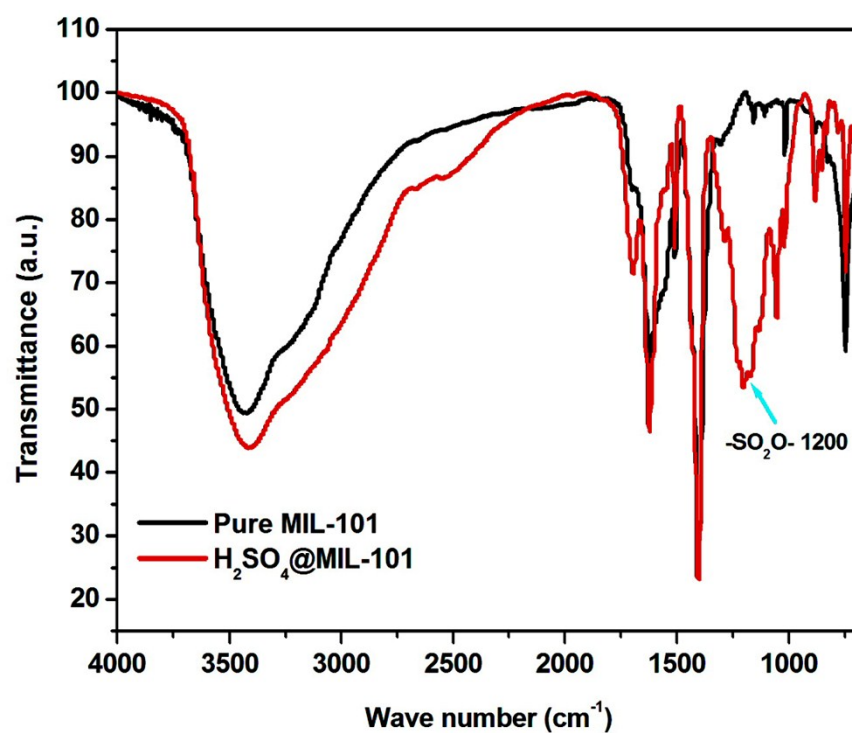


Fig. S8 Comparison of FT-IR spectra of H₂SO₄@MIL-101 with that of pure MIL-101 at room temperature.

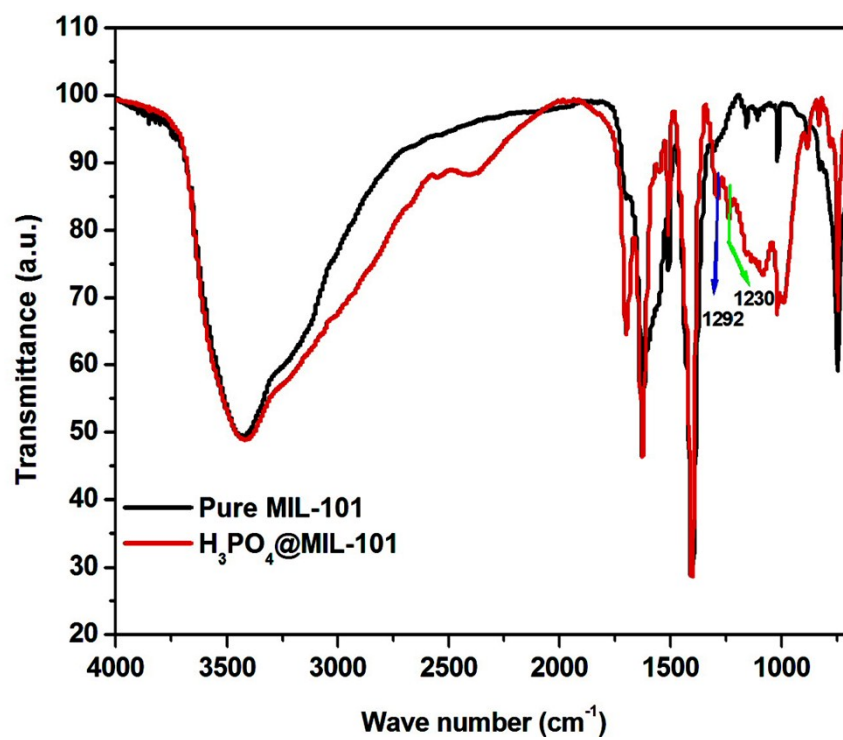


Fig. S9 Comparison of FT-IR spectra of H₃PO₄@MIL-101 with that of pure MIL-101 at room temperature.

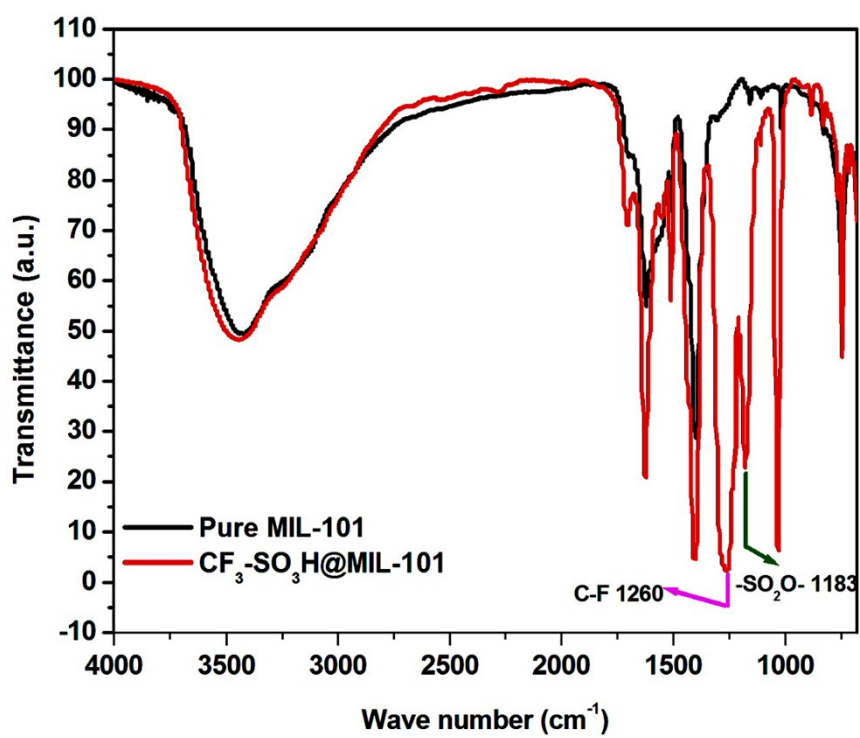


Fig. S10 Comparison of FT-IR spectra of CF₃SO₃H@MIL-101 with that of pure MIL-101 at room temperature.

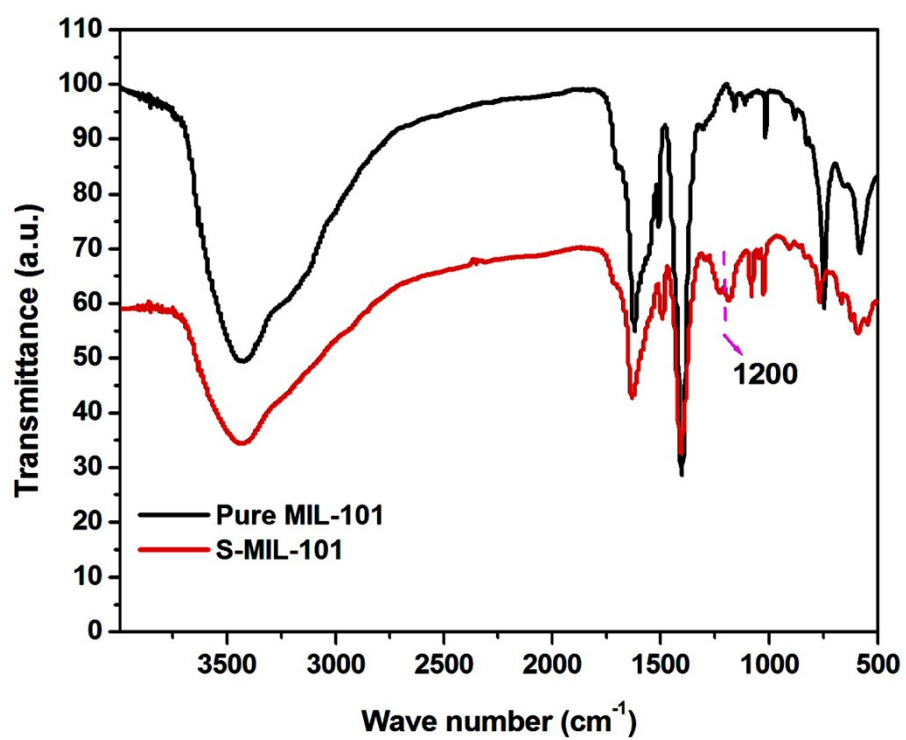


Fig. S11 Comparison of FT-IR spectra of S-MIL-101 with that of pure MIL-101 at room temperature.

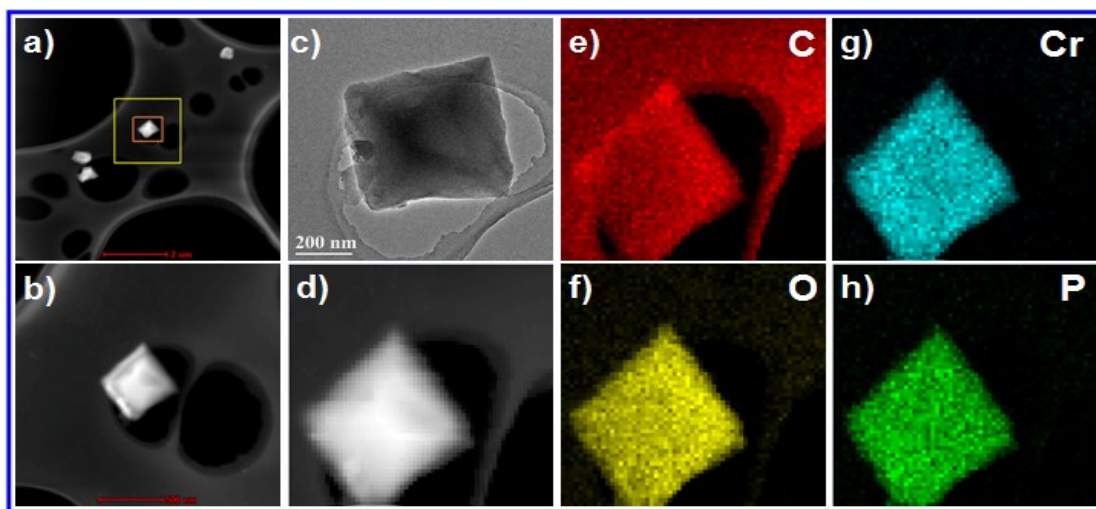


Fig. S12 Characterization EDS mapping of H₃PO₄@MIL-101 probed by: (a)(b)(c) FETEM image of H₃PO₄@MIL-101; (d) STEM image display of HAADF detector; (e) distribution of carbon; (f) distribution of oxygen; (g) distribution of chromium; (h) distribution of phosphorus.

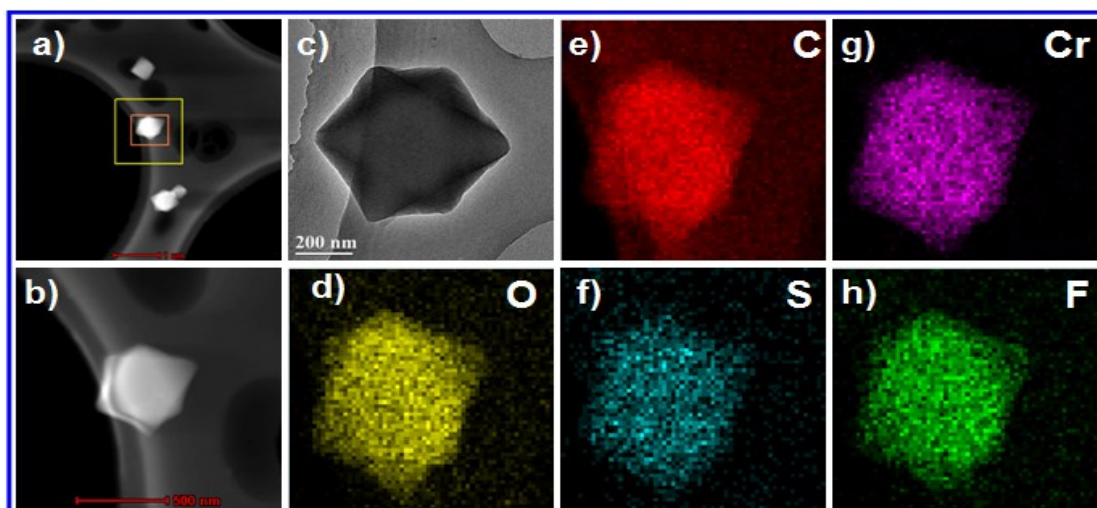


Fig. S13 Characterization of $\text{CF}_3\text{SO}_3\text{H@MIL-101}$ probed by EDS-mapping: (a)(b) (c)FETEM image of $\text{CF}_3\text{SO}_3\text{H@MIL-101}$; (d) distribution of oxygen; (e) distribution of carbon; (f) distribution of sulfur; (g) distribution of chromium; (h) distribution of fluorine.

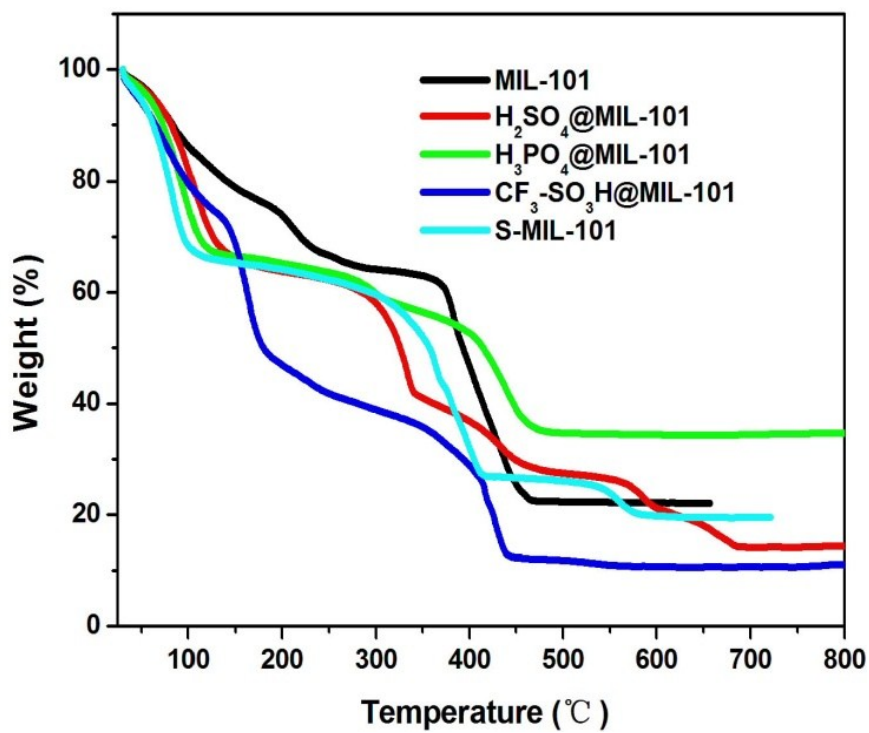


Fig. S14 The TGA curves of MIL-101, H₂SO₄@MIL-101, H₃PO₄@MIL-101, CF₃SO₃H@MIL-101 and S-MIL-101.

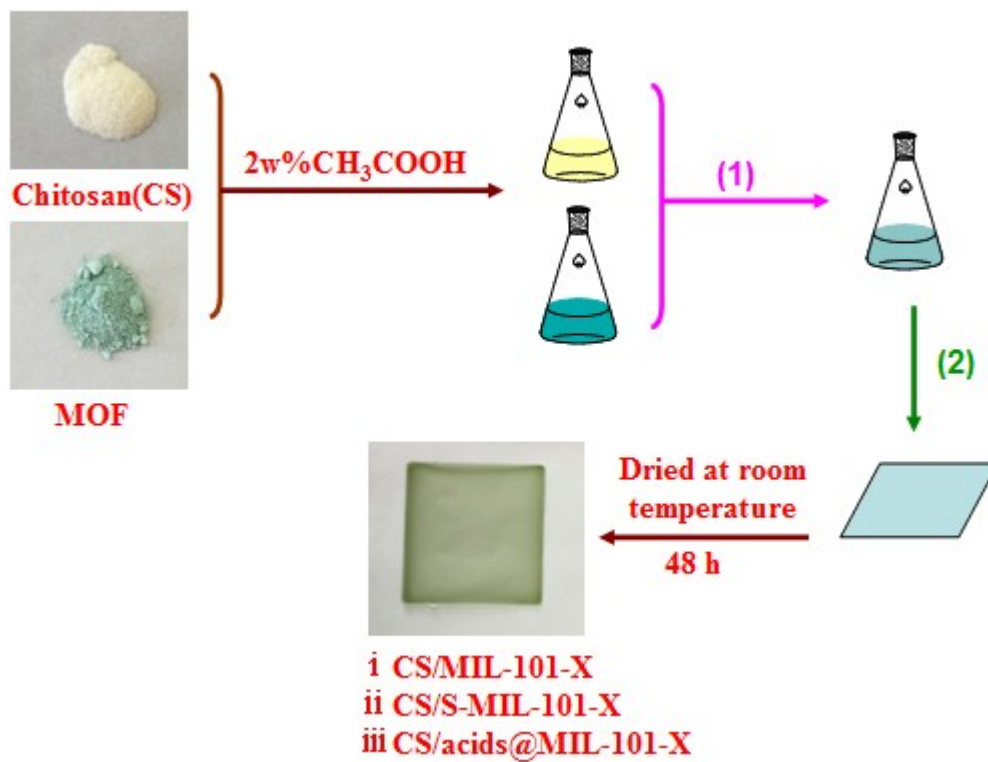


Fig. S15 The diagram of the process of CS/MIL-101-X, CS/S-MIL-101-X and CS/acids@MIL-101-X membranes preparation.

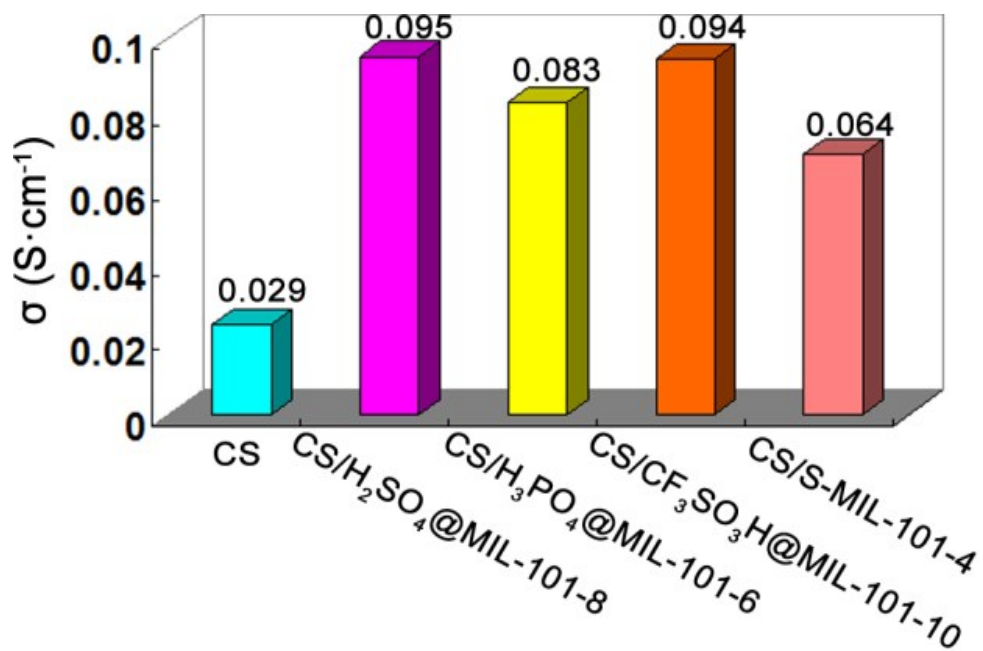


Fig. S16 Proton conductivity for various hybrid membranes at 100 °C and 100% RH.

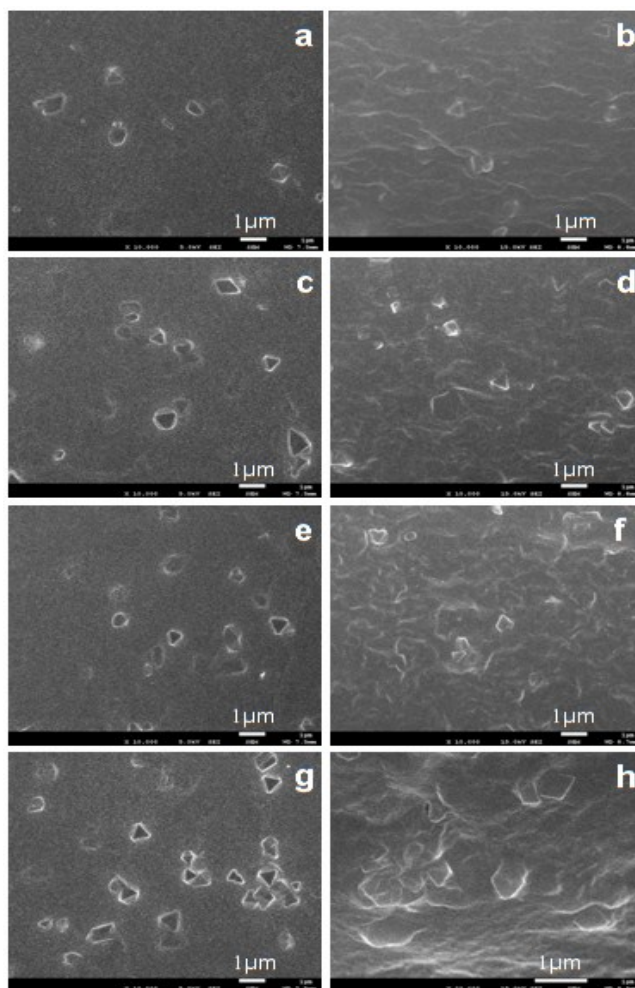


Fig. S17 FESEM images of the hybrid membranes: surface and cross-section of CS/MIL-101-3 (a)(b), CS/MIL-101-6 (c)(d), CS/MIL-101-12 (e)(f) and CS/MIL-101-21 (g)(h).

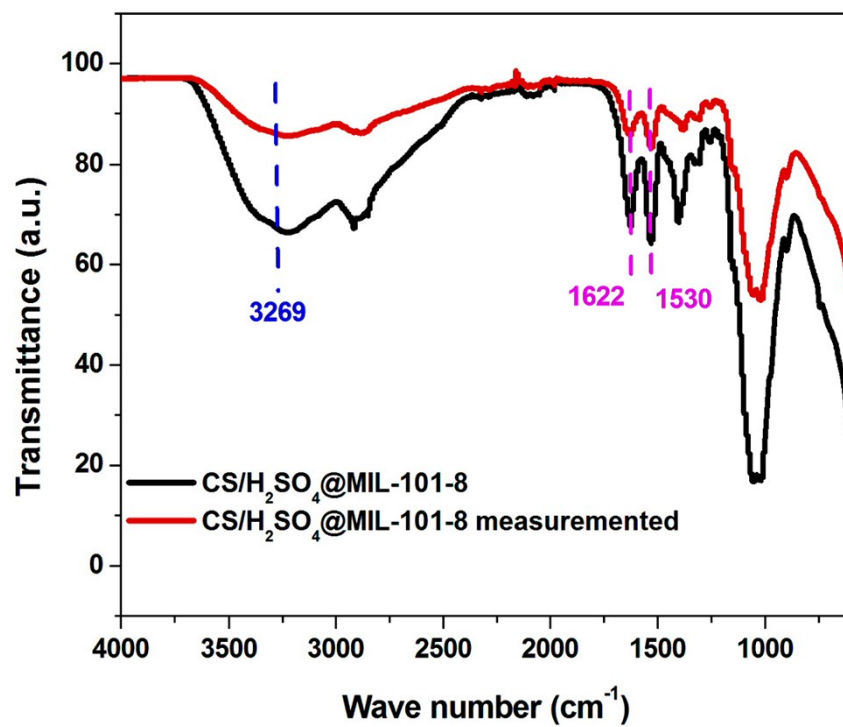


Fig. S18 IR spectra of CS/H₂SO₄@MIL-101-10 before and after the measurement of impedance at room temperature.

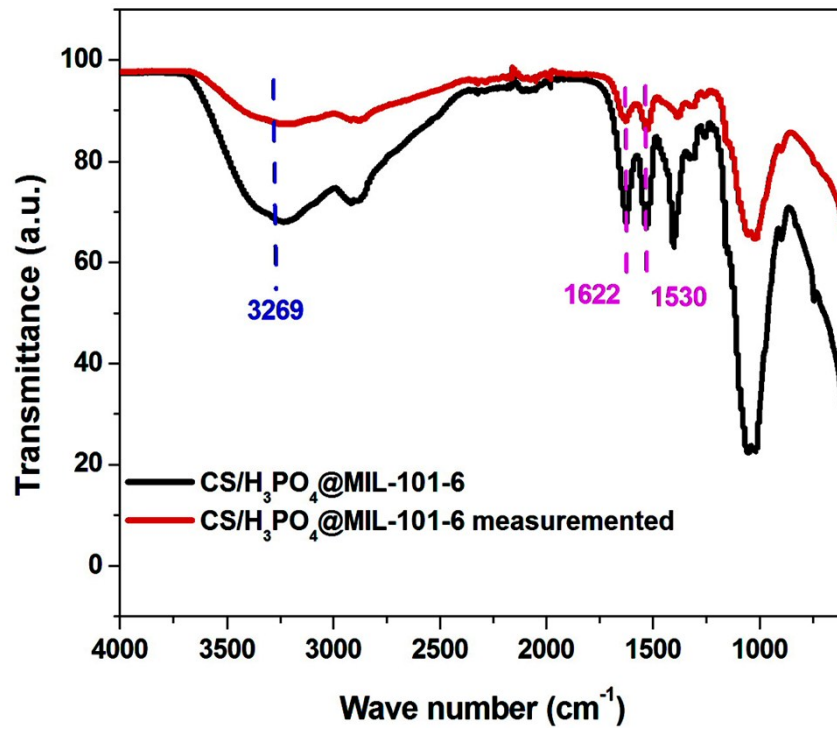


Fig. S19 IR spectra of the hybrid membrane CS/H₃PO₄@MIL-101-6 before and after the measurement of impedance at room temperature.

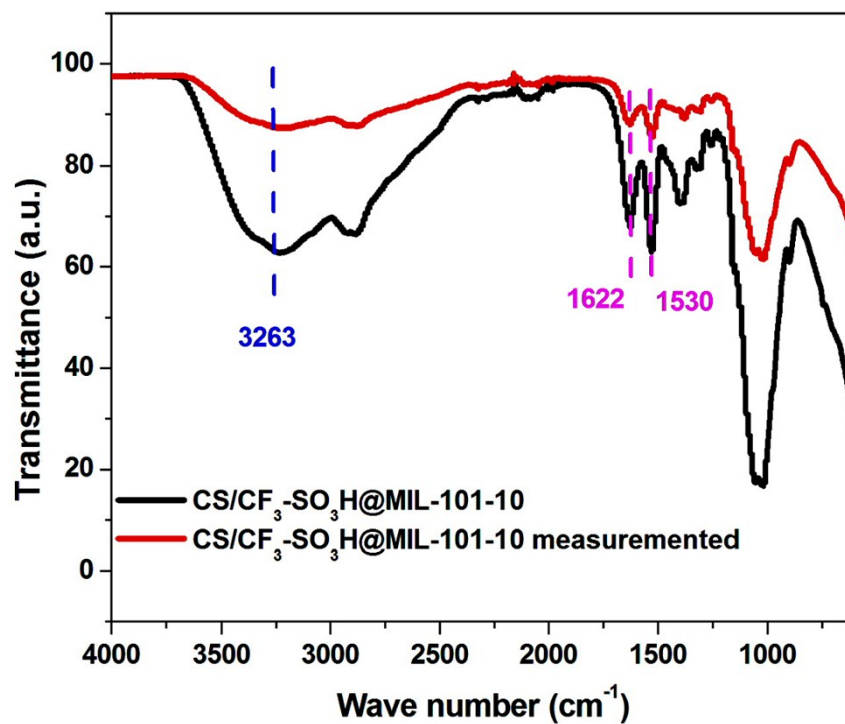


Fig. S20 IR spectra of the hybrid membrane CS/CF₃SO₃H@MIL-101-10 before and after the measurement of impedance at room temperature.

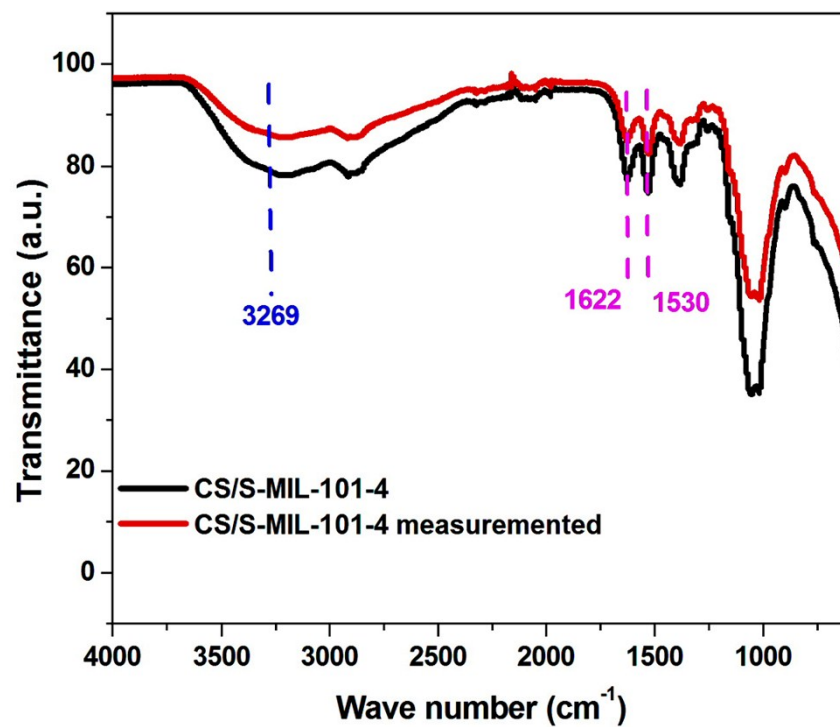


Fig. S21 IR spectra of the hybrid membrane CS/S-MIL-101-4 before and after the measurement of impedance at room temperature.

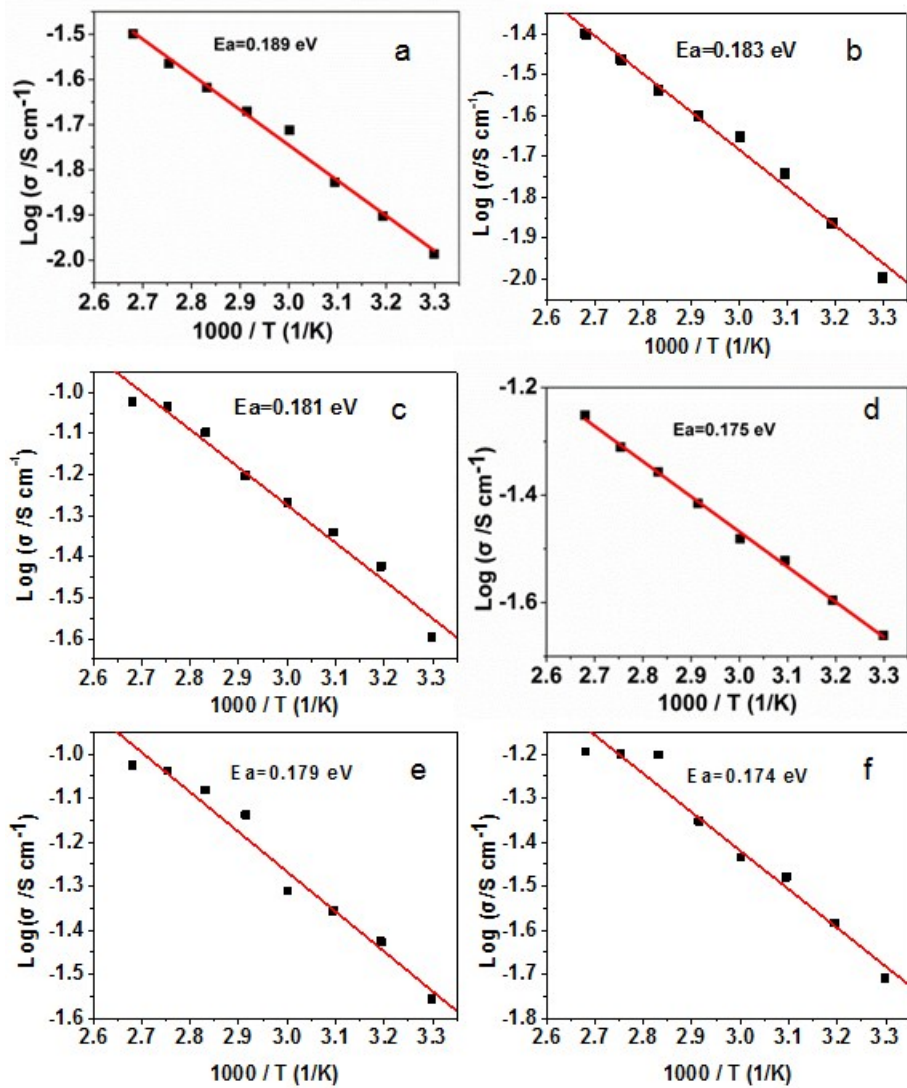


Fig. S22 Arrhenius plots of the conductivity of the membranes: (a) CS, (b) CS/MIL-101-12, (c) CS/ H_2SO_4 @MIL-101-8, (d) CS/ H_3PO_4 @MIL-101-6, (e) CS/ $\text{CF}_3\text{SO}_3\text{H}$ @MIL-101-10 and (f) CS/S-MIL-101-4.

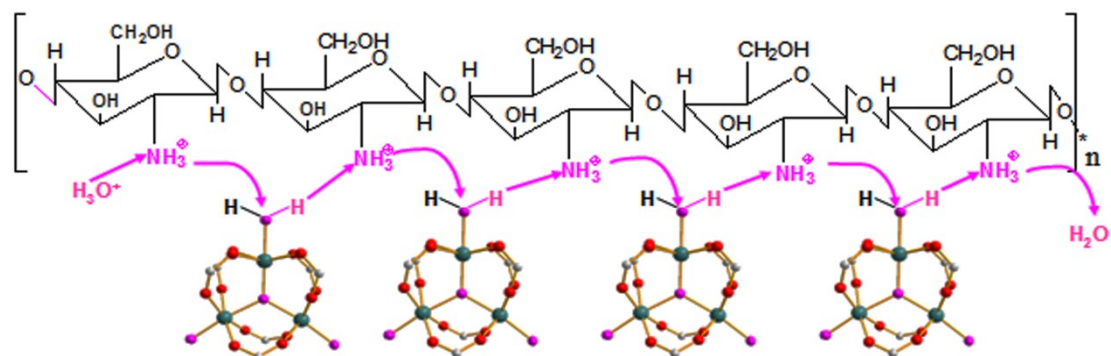


Fig. S23 Schematic illustration of the possible pathway of proton transfer in the CS/MIL-101-12 hybrid membrane.

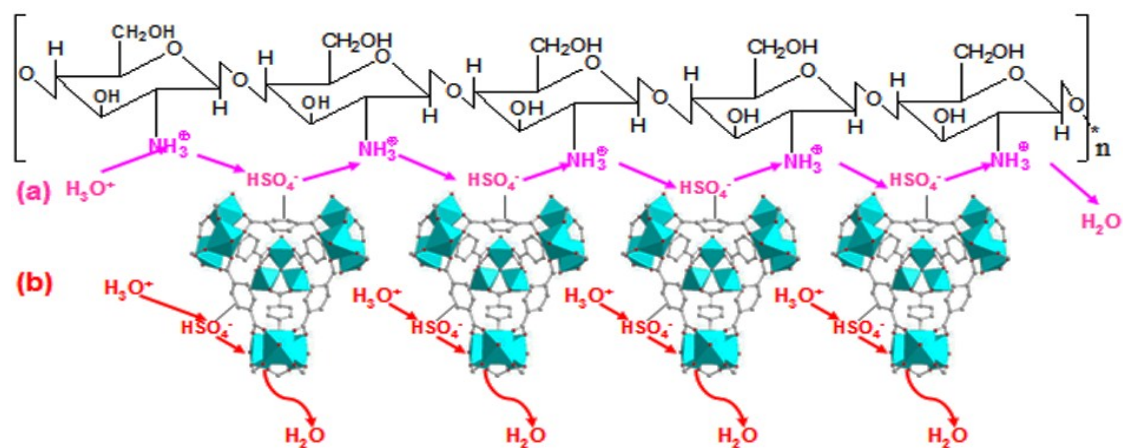


Fig. S24 Schematic illustration of the possible pathway of proton transfer in the CS/H₂SO₄@MIL-101-8 hybrid membrane.

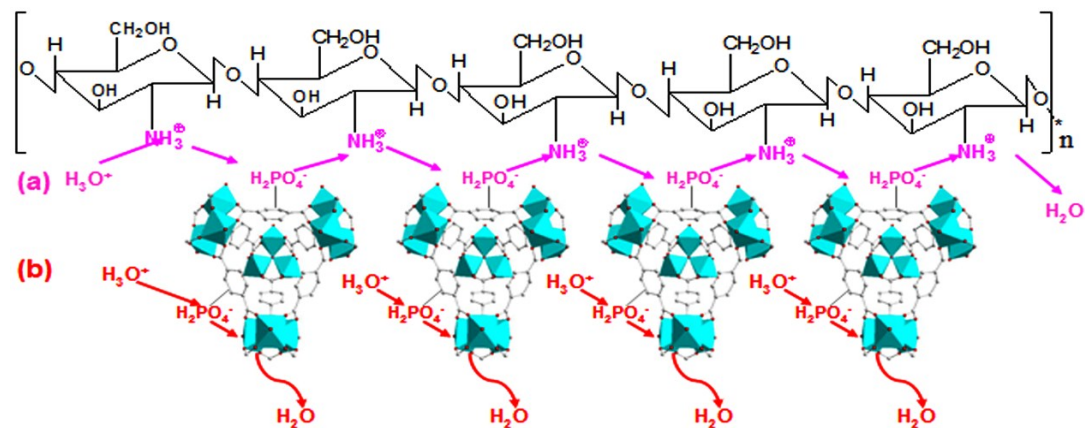


Fig. S25 Schematic illustration of the possible pathway of proton transfer in the CS/ H_3PO_4 @MIL-101-6 hybrid membrane.

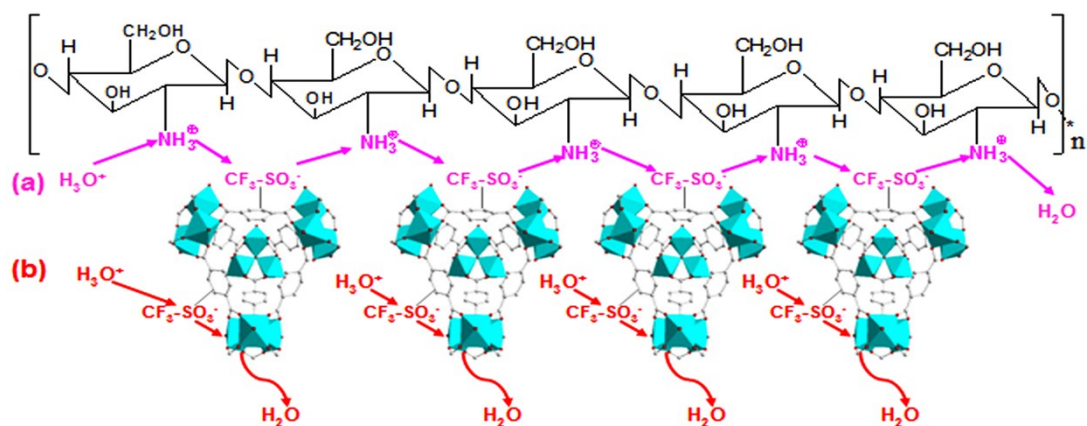


Fig. S26 Schematic illustration of the possible pathway of proton transfer in the CS/ CF_3SO_3H @MIL-101-10 hybrid membrane.

Table S1: Compare proton conductivity of five composite proton exchange membranes in this work with that of some MOF matrix composite membranes.

composite membrane	Prominent features/ guest	$\sigma / \text{S cm}^{-1}$	RH / (%)	T / (°C)
CS/MIL-101-12 (in this work)	Nitrogen atoms from $-\text{NH}_2$ groups line channels / lattice water	3.4×10^{-2}	100	100
CS/S-MIL-101-4 (in this work)	Nitrogen atoms from $-\text{NH}_2$ and Oxygen atoms from SO_3^- on the pore surface / water	6.4×10^{-2}	100	100
CS/H_2SO_4@MIL-101-8 (in this work)	Nitrogen atoms from $-\text{NH}_2$ and Oxygen atoms from H_2SO_4 in backbone facilitate H- bonding / water	9.5×10^{-2}	100	100
CS/H_3PO_4@MIL-101-6 (in this work)	Nitrogen atoms from $-\text{NH}_2$ and Oxygen atoms from H_3PO_4 in backbone facilitate H- bonding / water	8.3×10^{-2}	100	100
CS/$\text{CF}_3\text{SO}_3\text{H}$@MIL-101-10 (in this work)	Nitrogen atoms from $-\text{NH}_2$ and Oxygen atoms from $\text{CF}_3\text{SO}_3\text{H}$ in backbone facilitate H- bonding / water	9.4×10^{-2}	100	100
Ca-MOF-PVP ¹	Oxygen atoms from $-\text{COOH}$, Nitrogen atoms from protonated tertiary amine and Oxygen atoms from H_2O in backbone facilitate H- bonding / water	2.8×10^{-5}	53	25
Fe-MIL-101- NH_2 -SPPO ²	Oxygen atoms from lattice water and Oxygen atoms from $-\text{S}=\text{O}$ line channels / water	0.1	100	25
		0.25	100	90

SPPO/NAPI@MIL ³	Oxygen atoms from lattice water and Oxygen atoms from –S=O line channels / NAPI	4.0×10^{-2}	15	160
		2.5×10^{-4}	25	25
Nafion/phytic@MIL ⁴	Fluorine atoms from Nafion and Oxygen atoms from phytic acid inside pores / lattice water	6.1×10^{-2}	57.4	80
		0.156	100	
SEBS/PIL@MIL ⁵	Nitrogen atoms from PIL and Oxygen atoms from lattice water inside pores / H ₂ O	3.6×10^{-2}	—	20
SPEEK/Sul-MIL-101 ⁶	Oxygen atoms from –SO ₃ , SPEEK and water / lattice water	0.31	100	75
Copper foil/HKUST-1 ⁷	Not quite clear	6.9×10^{-4}	98	25
Cu-TCPP nanofilm ⁸	Oxygen atoms from –COOH line channels nanosheet	3.9×10^{-3}	98	25

References:

- 1 X.-Q. Liang, F. Zhang, W. Feng, X.-Q. Zou, C.-J. Zhao, H. Na, C. Liu, F.-X. Sun and G.-S. Zhu, *Chem. Sci.*, 2013, **4**, 983.
- 2 B. Wu, X.-C. Lin, L. Ge, L. Wu and T.-W Xu, *Chem. Commun.*, 2013, **49**, 143.
- 3 B. Wu, L. Ge, X.-C. Lin, L. Wu, J.-Y. Luo and T.-W Xu, *J. Membrane Sci.*, 2014, **458**, 86.
- 4 Z. Li, G.-W. He, B. Zhang, Y. Cao, H. Wu, Z.-Y Jiang and T.-T Zhou, *ACS Appl. Mater. Interfaces*, 2014, **6**, 979.
- 5 Z. Li, W.-Y. Wang, Y.-J. Chen, C.-Y. Xiong, G.-W. He, Y. Cao, H. Wu, M.-D. Guiver and Z.-Y. Jiang, *J. Mater. Chem. A*, 2016, **4**, 2340.
- 6 Z. Li, G.-W. He, Y.-N. Zhao, Y. Cao, H. Wu, Y.-F. Li, Z.-Y. Jiang, *Journal of Power Sources*, 2014, **262**, 372.
- 7 C. Xiao, Z.-Y. Chu, X.-M. Ren, T.-Y. Chen and W.-Q. Jin, *Chem. Commun.*, 2015, **37**, 7947.
- 8 G. Xu, K. Otsubo, T. Yamada, S. Sakaida and H. Kitagawa, *J. Am. Chem. Soc.*, 2013, **135**, 7438.